Geotechnical Testing Journal

Vahid Marefat,[1,2] François Duhaime,[2] Robert P. Chapuis,[3] and Vincent Le Borgne[4]

DOI: 10.1520/GTJ20170290

Performance of Fully Grouted Piezometers under Transient Flow Conditions: Field Study and Numerical Results

Geotechnical Testing Journal

doi:10.1520/GTJ20170290 available online at www.astm.org

Vahid Marefat,[1,2] François Duhaime,[2] Robert P. Chapuis,[3] and Vincent Le Borgne[4]

Performance of Fully Grouted Piezometers under Transient Flow Conditions: Field Study and Numerical Results

Reference

Marefat, V., Duhaime, F., Chapuis, R. P., and Borgne, V. L., "Performance of Fully Grouted Piezometers under Transient Flow Conditions: Field Study and Numerical Results," *Geotechnical Testing Journal* https://doi.org/10.1520/GTJ20170290.
ISSN 0149-6115

Manuscript received August 28, 2017; accepted for publication February 12, 2018; published online September 5, 2018.

[1] Department CGM, École Polytechnique de Montréal, PO Box 6079, Station CV, Montreal, QC H3C 3A7, Canada (Corresponding author), e-mail: vahid.marefat@polymtl.ca, https://orcid.org/0000-0002-1565-7852

[2] Laboratory for Geotechnical and Geoenvironmental Engineering (LG2), École de technologie supérieure, 1100 Notre-Dame Ouest, Montreal, QC H3C 1K3, Canada, https://orcid.org/0000-0001-8289-5837 (F.D.)

[3] Department CGM, École Polytechnique de Montréal, PO Box 6079, Station CV, Montreal, QC H3C 3A7, Canada, https://orcid.org/0000-0002-7397-9374

[4] GKM Consultants, 2141 Rue Nobel, Sainte-Julie, Quebec J3E 1Z9, Canada

ABSTRACT

Piezometers can be installed in clay layers using the fully grouted method. This method is said to reduce installation costs and facilitate installation, especially for nested piezometers. The success of a fully grouted installation depends upon the ratio of grout and surrounding soil hydraulic conductivity and upon the grout physical stability. This article presents new results from field tests and numerical simulations regarding the performance of fully grouted piezometers under transient flow conditions. The field observations show that using low-permeability grout for piezometer installation provides precise pore water pressure (PWP) measurements. This confirms previous findings on the fully grouted installation technique. Field observations for a very high-permeability grout that could be more than 1,100 times more permeable than the soil result in PWPs that totally differ from the PWP obtained with a low-permeability grout. Using three scenarios involving transient flow, the numerical results show that hydraulic conductivity ratios between 0.001 and 10 provide an accurate pore pressure response without a significant time lag for soils with a very low permeability ($K \leq 2 \times 10^{-9}$ m/s). For most practical applications, a hydraulic conductivity ratio of 100 is the upper limit to obtain acceptable pore pressure measurements for these soils. A large hydraulic conductivity ratio may cause a hydraulic short circuit between the fully grouted piezometer and the upper aquifer. For a borehole diameter of 100 mm, the numerical results demonstrate that grout stiffness has no significant impact on the performance of fully grouted piezometers. However, grout stiffness is important for the long-term performance of the fully grouted piezometer. This article also introduces preliminary results regarding a testing program on grout properties. These results confirm pervious findings by others that the preparation of low-permeability grout is not trivial and that grout initial viscosity controls its physical stability and hydraulic conductivity.

Keywords

pore pressure, cement-bentonite grout, fully grouted piezometer, field experiment, numerical modeling, low-permeability soil

Nomenclature

E = Young's modulus (MPa)
E_s = Young's modulus of soil (MPa)
E_g = Young's modulus of grout (MPa)
ε = normalized error (%)
γ = unit weight of soil (kN/m^3)
K = hydraulic conductivity (m/s)
K_s = hydraulic conductivity of soil (m/s)
K_g = hydraulic conductivity of grout (m/s)
m_v = compressibility (kPa^{-1})
m_{vs} = compressibility of soil (kPa^{-1})
m_{vg} = compressibility of grout (kPa^{-1})
θ = volumetric water content (−)
u_t^* = pore pressure measured with reference piezometer (kPa)
u_{fgt} = pore pressure measured with fully grouted piezometer (kPa)
ν = Poisson's ratio (−)

Introduction

The fully grouted installation method for piezometers entails lowering a piezometer in a borehole that is backfilled with grout, without using a filter pack. The main advantages of this method are its reduced cost and ease of installation, especially when several instruments are installed in the same borehole. Therefore, the fully grouted method can be much less expensive than traditional installations with sand pack and can save around 75 % of the installation cost (McKenna 1995).

The fully grouted installation method for vibrating wire pressure transducers (VWPs) has recently received much interest in mining, geotechnical engineering, and hydrogeology. In mining, VWPs installed with the fully grouted technique are commonly used to monitor hydraulic head fluctuations caused by underground mining activities (e.g., Yungwirth et al. 2013; Zawadzki and Chorley 2014). In geotechnical engineering, fully grouted piezometers are installed within clay layers to monitor the consolidation caused by earth structures such as embankments or tailing dams (Contreras, Grosser, and Ver Strate 2011). They are also installed to monitor natural slope stability (Simeoni et al. 2011), excavations in urban areas (Jurado et al. 2012; Pujades et al. 2012, 2014), and ground response to tunnelling (Wan and Standing 2014). In hydrogeology, fully grouted piezometers are deployed in clay aquitards for baseline monitoring of natural pore water pressure (PWP) fluctuations (Smith, van der Kamp, and Hendry 2013; Smerdon et al. 2014).

Even if the fully grouted installation method has spread throughout the world, its reliability is still questioned, particularly when it is used to measure PWP changes in soils with a very low permeability. Piezometer efficiency can be defined by measurement accuracy and time lag (McKenna 1995). Time lag represents the time taken by the piezometer to reach its equilibrium pressure following a pore pressure change in the area surrounding the sensor (Hvorslev 1951). Deviation of the measured PWP from the real PWP of the natural soil before drilling is called the piezometric error. This deviation may be due to several factors, most importantly the grout properties.

Previous studies on the field performance of fully grouted piezometers (McKenna 1995; DeJong et al. 2004; Contreras, Grosser, and Ver Strate 2007, 2011, 2012; Simeoni et al. 2011; Wan and Standing 2014) and reduced scale laboratory conditions (Mikkelsen 2000; Bayrd 2011; Simeoni 2012; Contreras, Grosser, and Ver Strate 2012) demonstrated that fully grouted piezometers work successfully if an appropriate grout is used for piezometer sealing. Several authors have claimed that the grout hydraulic conductivity, K_g, is the main parameter that influences the performance of fully grouted piezometers (Vaughan 1969; McKenna 1995; Mikkelsen and Green 2003; Contreras, Grosser, and Ver Strate 2008). A few authors have tried to prove that a grout that is more permeable than the target formation can lead to a negligible piezometric error in some cases (Vaughan 1969; Contreras, Grosser, and Ver Strate 2007, 2008).

For steady-state seepage conditions, the analytical solution of Vaughan (1969) indicated that the grout could be two orders of magnitude more permeable than the surrounding formation without inducing an appreciable piezometric error. In addition, a simple numerical simulation by Contreras, Grosser, and Ver Strate (2008) revealed that the normalized error was 0 up to a permeability ratio of 1,000. Mikkelsen (2002) qualitatively proposed a permeability ratio up to 100 for a precise pore pressure measurement. On the other hand, a field study led McKenna (1995) to conclude that for most soils, the grout must be less permeable than the surrounding ground to minimize the piezometric error.

It would be interesting to know the piezometric error and time lag induced by grouts with different properties (K_g and m_{vg}) under various field conditions. This would help to evaluate the capacity of the fully grouted method to obtain precise PWP measurements in diverse settings. There is no agreement on the maximum permeability ratio (K_g/K_s) for fully grouted piezometer installations in previous works. In addition, the fully grouted installation method for VWPs is not included in any ASTM standard. The first objective of this article is to present the field performance of two sets of fully grouted piezometers sealed with two grouts of very high and low permeabilities in Sainte-Marthe, near Montreal, Canada. Previous works have not investigated the field performance of a fully grouted piezometer sealed with such a high-permeability grout ($K_g/K_s \geq 1{,}000$). The second objective is to model the response of fully grouted piezometers to groundwater level changes and to external loadings using practical numerical simulations.

Materials and Methods

This section first presents the installation of the two sets of fully grouted piezometers sealed in massive Champlain clay in Sainte-Marthe, near Montreal, Canada. Then, the methodology for the numerical modeling of the fully grouted piezometers will be presented.

FIELD INSTALLATION OF FULLY GROUTED PIEZOMETERS

The study site is located in Sainte-Marthe, south of Highway 40, west of road 201, and east of road 325. On the study site, the intact Champlain clay is located under a layer of stiff brownish clay, which is sometimes oxidized and fractured. The fracture depths can reach up to 6 m from the ground surface. The intact clay deposit has a thickness of around 10 m. In the lower portion, the clay is mixed with sand, silt, and coarser material, including some local blocks. The intact clay deposit is soft and sensitive at depths between 6 and 10 m. Sensitivity can reach 200 at a depth of around 10 m. The silty layer is underlain by the bedrock, which is sometimes fractured at the interface with the silty layer. Falling-head laboratory tests on intact clay specimens provided an average K value of 1.08×10^{-9} m/s for the Sainte-Marthe clay. This value falls within the typical range for Champlain clays (5×10^{-10} to 5×10^{-9} m/s), as reported previously in Tavenas et al. (1983a, 1983b), Duhaime (2012), and Duhaime and Chapuis (2014). **Fig. 1** presents a geotechnical profile for the study site.

Three boreholes labeled F1, F2, and F3 were drilled in October 2016 using a wash boring technique, with a flush-joint straight casing. The three boreholes have a diameter of 114 mm. During borehole drilling, the clay layer was sampled using thin-wall tube samplers at an interval of 1.5 m. **Fig. 2** shows a cross section of the piezometer installation. Boreholes F1 and F2 were drilled down into the bedrock (22 m from the ground surface), while borehole F3 was drilled only to the lower third of the clay layer (12.5 m from the ground surface). Two monitoring wells (MWs) were installed in boreholes F1 and F2. The centers of the MWs' intake zones were located at a depth of 21 m below the ground surface at the interface between the fractured bedrock and the silty layer. In each borehole, two multilevel piezometers were installed approximately at the lower and upper thirds of the clay layer. Boreholes F1 and F3 each include two VWPs, which were fully grouted at depths of 6.1 m (F1A and F3A) and 12.2 m (F1B and F3B) below the ground surface. These VWPs have a full-scale reading range of 350 kPa and a resolution of 1 mm of water. Borehole F2 contains two standpipe piezometers with a riser pipe diameter of 21 mm and a sand filter around the piezometer tips. The center of the intake zones for the standpipe piezometers

FIG. 1

Geotechnical profile for the study site. w_L, liquid limit; w_p, plastic limit; w_n, natural water content; C_u, undrained shear strength.

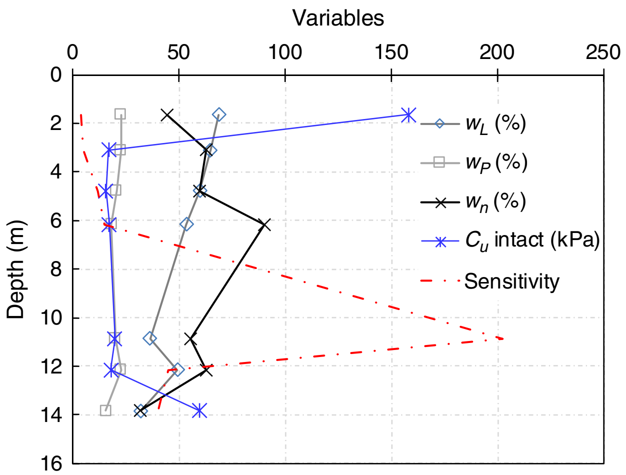

FIG. 2

Cross-sectional sketch of the boreholes and piezometers.

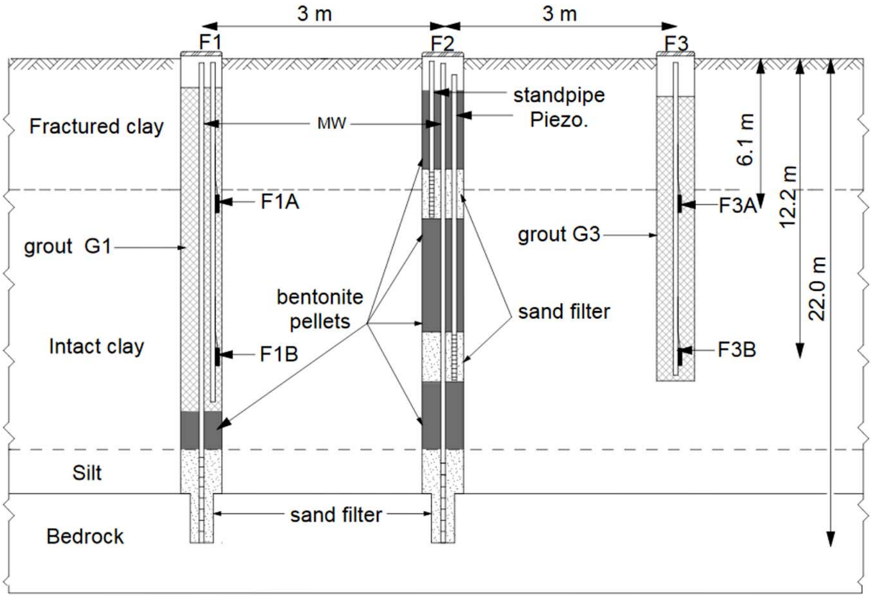

was located approximately at the same depth as the VWPs (**Fig. 2**). The approximate length and diameter of the sand filters were 457 and 114 mm, respectively.

For the installation, once the boreholes were drilled and washed clean, the VWPs were attached to a ¾-in. grout pipe, which was lowered in the borehole down to the proper depth. The grout pipe supported the installation weight and conveyed the grout from the mixer to the borehole. After having positioned the piezometer assembly in the borehole, the hole was grouted from the bottom up. The current basic grout recipe for soft soils as suggested by Mikkelsen (2002) in weight proportions is 6.5 parts water: 1 part cement: 0.4 part bentonite. This recipe is an initial guide. The bentonite content must be adjusted until a "thick cream or pancake batter"–like grout is obtained (Mikkelsen 2002). Adding more bentonite increases grout viscosity and results in a physically stable grout. However, a viscous grout is more difficult to pump and does not flow easily into narrow spaces, for example, between the piezometer cable, the grout pipe, and the casing. Therefore, an appropriate consistency is needed to produce not only a physically stable grout but also a pumpable grout. Contreras, Grosser, and Ver Strate (2007) proposed a Marsh Funnel viscosity between 50 and 60 s for a stable grout. After adjusting the grout consistency with additional bentonite, an average hydraulic conductivity (K_g) of 7.2×10^{-8} m/s was reported in Contreras, Grosser, and Ver Strate (2007, 2008) for the aforementioned recipe. Given an average K_s of 1.08×10^{-9} m/s for the Sainte-Marthe clay, one may expect a permeability ratio around 70 between the grout and the surrounding clay.

The fieldwork in this study investigates the response of fully grouted piezometers sealed with two grouts of low and very high permeabilities (K_g/K_s ratios of around 1 and 1,000, respectively). Therefore, two different grouts were used to seal the VWPs in boreholes F1 and F3. The grout for F3, later identified as G3, corresponds to the basic grout recipe as suggested by Mikkelsen (2002) for soft soil (6.5 parts water: 1 part cement: 0.4 part bentonite). Contrarily to the recommendations of Mikkelsen (2002) and

Contreras, Grosser, and Ver Strate (2007, 2008), the grout consistency was not adjusted with additional bentonite in order to produce a very high-permeability grout. For borehole F1A, a new grout recipe (G1) was designed. The solid content and cement/bentonite ratio in recipe G1 were higher than those in recipe G3 in order to produce a low-permeability grout. The weight proportions for the new recipe were 5 parts water for 1 part cement and 1.2 part bentonite. The higher solid and bentonite contents made grout G1 more viscous and more difficult to pump down into the borehole through the grout pipe. Therefore, a liquid and chloride-free superplasticizer (SP) was added in recipe G1 in order to increase the grout flowability. The concentration of SP was about 2.0 % of the solid weight.

The bentonite used in this study was standard 200 mesh (Opta Minerals) and the cement was a general purpose hydraulic cement. Tap water from the city of Sainte-Marthe was used. Materials were weighted in the field with a portable balance. The water was first poured into a 150-L barrel and mixing was started. Then, the cement was slowly added to the water and mixed thoroughly. Next, bentonite powder was gradually added into the barrel to avoid forming clumps. The mixing duration of about 10–15 min depends upon the quantity of bentonite added in the mix.

Both grouts were sampled after grout mixing. The grout samples were left in the field to set for a week and then transferred to a controlled temperature and humidity chamber for further curing. Because extra bentonite was not added to grout G3, it was thin and not physically stable. After the setting period, approximately 25∼30 % of the mold heights and of borehole F3 annular space height were found to be empty because of the segregation of the unstable grout. The low grout viscosity (low bentonite content) was the reason for material separation (Contreras, Grosser, and Ver Strate 2007). The piezometer F3B was not fully open: a field evaluation revealed that there was still about 8 m of grout column on top of piezometer F3B. Falling-head laboratory tests were conducted on the two sets of hardened grout specimens based on ASTM D5084-16, *Standard Test Methods for Measurement of Hydraulic Conductivity of Saturated Porous Materials Using a Flexible Wall Permeameter*. They provided average K_g values of 6.1×10^{-9} and 1.2×10^{-6} m/s, respectively, for grouts G1 and G3. Further tests with the G3 recipe, but with four different brands of bentonite powder, provided K values between 1.37×10^{-6} and 3.7×10^{-6} m/s. It is important to note here that the grout consistency was not adjusted with additional bentonite (exact recipes were followed for grout mixing). Table 1 summarizes the recipes and properties for grouts G1 and G3. For a mean K_s value of 1.08×10^{-9} m/s for the Sainte-Marthe clay, permeability ratios of around 1,100 and 6 can be expected between grout and surrounding clay for grouts G3 and G1, respectively.

TABLE 1
Grout recipes, hydraulic conductivity, and compressibility.

Grout	Borehole F1		Borehole F3	
	G1		G3	
	M, kg	Ratio	M, kg	Ratio
Water	120	5	120	6.5
Cement	24	1	18.5	1
Bentonite	28	1.2	7.5	0.4
SP (% of solid)	2		0	
K, m/s	6.1×10^{-9}		1.2×10^{-6}	
m_v, kPa^{-1}	4.15×10^{-5}		5.9×10^{-5}	

NUMERICAL SCENARIOS

The numerical models assume a perfect installation and ignore any error related to drilling or installation. They examine the influence of grout properties (i.e., K_g and m_{vg}) on the PWP response measured with fully grouted piezometers. These scenarios include the response of fully grouted piezometers to

- rapid (1-day) pore pressure changes,
- seasonal groundwater table fluctuations, and
- external loading (total stress change).

Various types of soil and grout were assumed in the numerical simulations. For each scenario, the PWP response was calculated for a series of piezometers sealed with several types of grout to a depth of 5 m along the borehole centerline. The response of each fully grouted piezometer was then compared to the response of a reference (perfect) piezometer. The reference piezometer corresponds to the PWP modeled in the soil without the installation of a piezometer. The numerical scenarios considered a horizontal, saturated, isotropic, and homogenous clay layer. The normalized error (ε) induced by the grout properties at a given time t is expressed as a percentage of the reference piezometer response as follows:

$$\varepsilon = \frac{u_{tfg} - u_t^*}{u_t^*} \times 100 \tag{1}$$

where u_t^* is the reference PWP at time t and u_{tfg} is the PWP measured by the fully grouted piezometer at time t. The normalized error defined by Eq 1 tells us about the relative efficiency of different grouts. It should be noted that ε is biased with regard to the formation hydraulic head/PWP, or the reference system for the hydraulic head values. Different hydraulic head datums and boundary conditions will result in different normalized errors.

Fully Grouted Piezometer Response to a 1-Day Change in Groundwater Level

This scenario studies the PWP response caused by a 1-day change in the hydraulic head of an aquifer contiguous to the clay layer. The change in the hydraulic head slowly propagates everywhere within the low-permeability soil layer (Chapuis 2009). The finite-element code SEEP/W (GEO-SLOPE International 2012) was used for simulating the PWP response to changes in groundwater levels at the upper and lower boundaries (aquifers). SEEP/W solves Darcy's law for seepage and the complete Richards' (1931) equation for mass conservation of water. The numerical model is an axisymmetric model with a height of 10 m and a radius of 20 m. The model includes a borehole with a diameter of 100 mm. The borehole penetrates within the soil layer over a depth of 5.10 m. The VWPs were sealed at the borehole centerline, 10 cm above its bottom (Fig. 3). For transient seepage problems, SEEP/W requires hydraulic conductivity (K) and compressibility (m_v) values for each of the simulated materials. The available data in the literature provide values for K_g ranging between 8×10^{-8} and 1×10^{-10} m/s (e.g., McKenna 1995; Contreras, Grosser, and Ver Strate 2007, 2008). In this study, the lower and upper bounds of the applicable range for K_g and m_{vg} were selected based on the preliminary results of a laboratory testing program on cement-bentonite grouts that is currently being conducted at École de technologie supérieure by the authors. Table 2 summarizes preliminary lower and upper bounds of K_g

FIG. 3

Cross section of the numerical model, including the fully grouted borehole.

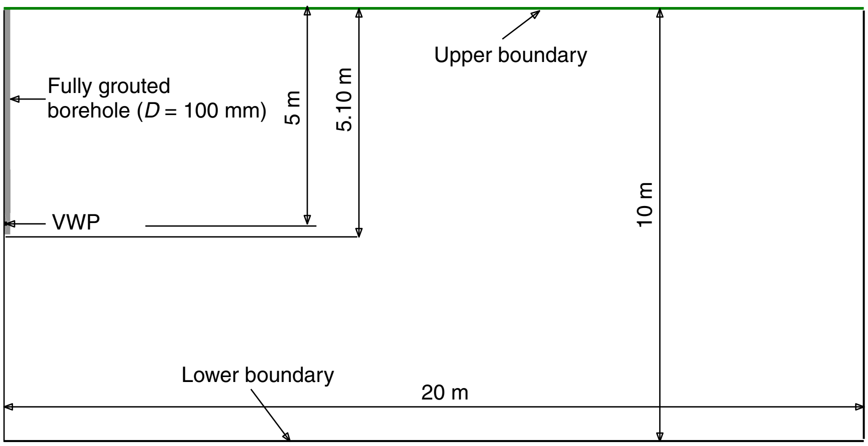

TABLE 2

Lower and upper bounds for K_g and m_{vg} for pumpable grouts.

	Material-Weight Ratio					
Grout	Water	Cement	Bentonite	SP, % of solid	K_g, m/s	m_{vg}, kPa^{-1}
1	2.5	1	0.63	2	2.60×10^{-10}	1.20×10^{-6}
2	6.5	1	0.4	0	2.16×10^{-6}	1.23×10^{-4}

and m_{vg} for pumpable grouts obtained in this testing program. The m_{vg} values in Table 2 were obtained from consolidated undrained shear tests (ASTM D4767-11, *Standard Test Method for Consolidated Undrained Triaxial Compression Test for Cohesive Soils*).

The first scenario considers four types of soil with hydraulic conductivities (K_s) ranging between 2×10^{-7} and 2×10^{-10} m/s. The four soils were assumed to have an identical compressibility (m_{vs}) of 1.49×10^{-5} kPa^{-1} (equivalent to a Young's modulus, E_s, of 50 MPa with a Poisson's ratio, ν, of 0.3). For each soil, the VWPs were assumed to be fully grouted, with 15 grouts having K_g values ranging between 2×10^{-6} and 2×10^{-10} m/s and m_{vg} values ranging between 1.49×10^{-4} and 1.49×10^{-6} kPa^{-1} (E_g between 5 and 500 MPa, with $\nu = 0.3$). Table 3 summarizes the soil and grout properties that were used for this model.

The transient simulations were carried out in two steps. Step 1 consisted of a steady-state simulation, which was used as the initial condition for the transient simulation. It was thus considered that the VWP was initially at equilibrium with the PWP in the soil. During the steady-state simulation, arbitrary hydraulic head boundary conditions of 10.0 and 5.0 m were applied to the upper and lower boundaries of the model, respectively. These boundary conditions correspond to constant hydraulic head values in the aquifers located above and under the clay layer. In step 2, the hydraulic head was increased at a constant rate in 1 day from 10.0 to 11.5 m at the upper boundary of the clay layer. The hydraulic head value for the lower boundary of the model was kept constant at 5.0 m for step 2. After having conducted the convergence studies (Chapuis 2010, 2012a, 2012b, 2012c) and the sensitivity analysis, the response of the fully grouted piezometers to

TABLE 3
Soil and grout properties included in scenario 1.

Soil	K_s, m/s	m_{vs}, kPa^{-1}	G	K_g, m/s	m_{vg}, kPa^{-1}	G	K_g, m/s	m_{vg}, kPa^{-1}	G	K_g, m/s	m_{vg}, kPa^{-1}
1	2.0×10^{-10}	1.49×10^{-5}	1	2.0×10^{-10}	1.49×10^{-4}	6	2.0×10^{-10}	1.49×10^{-5}	11	2.0×10^{-10}	1.49×10^{-6}
2	2.0×10^{-9}	1.49×10^{-5}	2	2.0×10^{-9}	1.49×10^{-4}	7	2.0×10^{-9}	1.49×10^{-5}	12	2.0×10^{-9}	1.49×10^{-6}
3	2.0×10^{-8}	1.49×10^{-5}	3	2.0×10^{-8}	1.49×10^{-4}	8	2.0×10^{-8}	1.49×10^{-5}	13	2.0×10^{-8}	1.49×10^{-6}
4	2.0×10^{-7}	1.49×10^{-5}	4	2.0×10^{-7}	1.49×10^{-4}	9	2.0×10^{-7}	1.49×10^{-5}	14	2.0×10^{-7}	1.49×10^{-6}
–	–	–	5	2.0×10^{-6}	1.49×10^{-4}	10	2.0×10^{-6}	1.49×10^{-5}	15	2.0×10^{-6}	1.49×10^{-6}

Note: G = grout.

the 1-day change in groundwater level was simulated for up to 1,000 days, depending on the hydraulic conductivity of the modeled clay. More than 60 numerical simulations were conducted to assess the ε value for fully grouted piezometers.

The sensitivity of the numerical model for various soil and grout parameters as well as borehole geometry was studied. In the low-permeability soil ($K_s = 2\times10^{-10}$ m/s), two key parameters influence the equilibration of the pore pressure imbalance between the fully grouted piezometer and the surrounding clay layer (Fig. 4a and g). The numerical results are most sensitive to grout hydraulic conductivity and clay compressibility. On the other hand, the model results are insensitive to the grout compressibility and borehole diameter (Fig. 4c and e). In the high-permeability soil (Fig. 4b, d, f, and h), the results only display little sensitivity to the borehole diameter (Fig. 4f).

Fully Grouted Piezometer Response to Seasonal Groundwater Table Fluctuations

The second scenario looks at the response of fully grouted piezometers to seasonal fluctuations in the groundwater table. The model geometry and the simulation steps were the same as for scenario 1. For the initial condition, a constant hydraulic head of 10 m was applied to the model. On the other hand, the transient flow was initiated by applying a hydraulic head boundary condition corresponding to seasonal groundwater table changes at the top boundary of the soil. The applied seasonal groundwater fluctuations were based on field data obtained in the upper aquifer on the Sainte-Marthe study site between December 2016 and June 2017. The raw data represent the composite responses from various hydrogeological factors or events, or both, each with varying periods (frequencies) of stress application. The observed data were smoothed to avoid numerical issues related to sharp fluctuations in boundary conditions (Duhaime et al. 2017). This study used a fast Fourier transform low-pass filter with a cutoff frequency of 0.1 day^{-1} to remove the high-frequency noise from the observed raw data. The low-pass filter provides a “window” to pass signals with a frequency lower than a defined cutoff frequency.

Two types of low-permeability clay with K_s of 2×10^{-9} and 2×10^{-10} m/s were used for scenario 2. For each soil, five types of grout with K_g ranging between 2×10^{-6} and 2×10^{-10} m/s were modeled. All grouts had an identical compressibility (m_{vg}) of 1.49×10^{-5} kPa^{-1}. More than ten numerical simulations were conducted to assess the performance of fully grouted piezometers under a seasonal groundwater change. Table 4 summarizes the soil and grout properties for this model.

Fully Grouted Piezometer Response to an External Mechanical Loading

The third scenario concerns the response of a fully grouted piezometer to an external mechanical load. Fig. 5 presents a sketch of the fully grouted piezometer and loading

FIG. 4 Sensitivity of the numerical model to (a) grout hydraulic conductivity (low-permeability soil, $K_s = 2 \times 10^{-10}$ m/s), (b) grout hydraulic conductivity (high-permeability soil, $K_s = 2 \times 10^{-7}$ m/s), (c) grout compressibility (low-permeability soil, $K_s = 2 \times 10^{-10}$ m/s), (d) grout compressibility (high-permeability soil, $K_s = 2 \times 10^{-7}$ m/s), (e) borehole diameter (low-permeability soil and grout, $K_s = K_g = 2 \times 10^{-10}$ m/s), (f) borehole diameter (high-permeability soil, $K_s = 2 \times 10^{-7}$ m/s, and low-permeability grout, $K_g = 2 \times 10^{-10}$ m/s), (g) soil compressibility (low-permeability soil, $K_s = 2 \times 10^{-10}$ m/s), and (h) soil compressibility (high-permeability soil, $K_s = 2 \times 10^{-7}$ m/s).

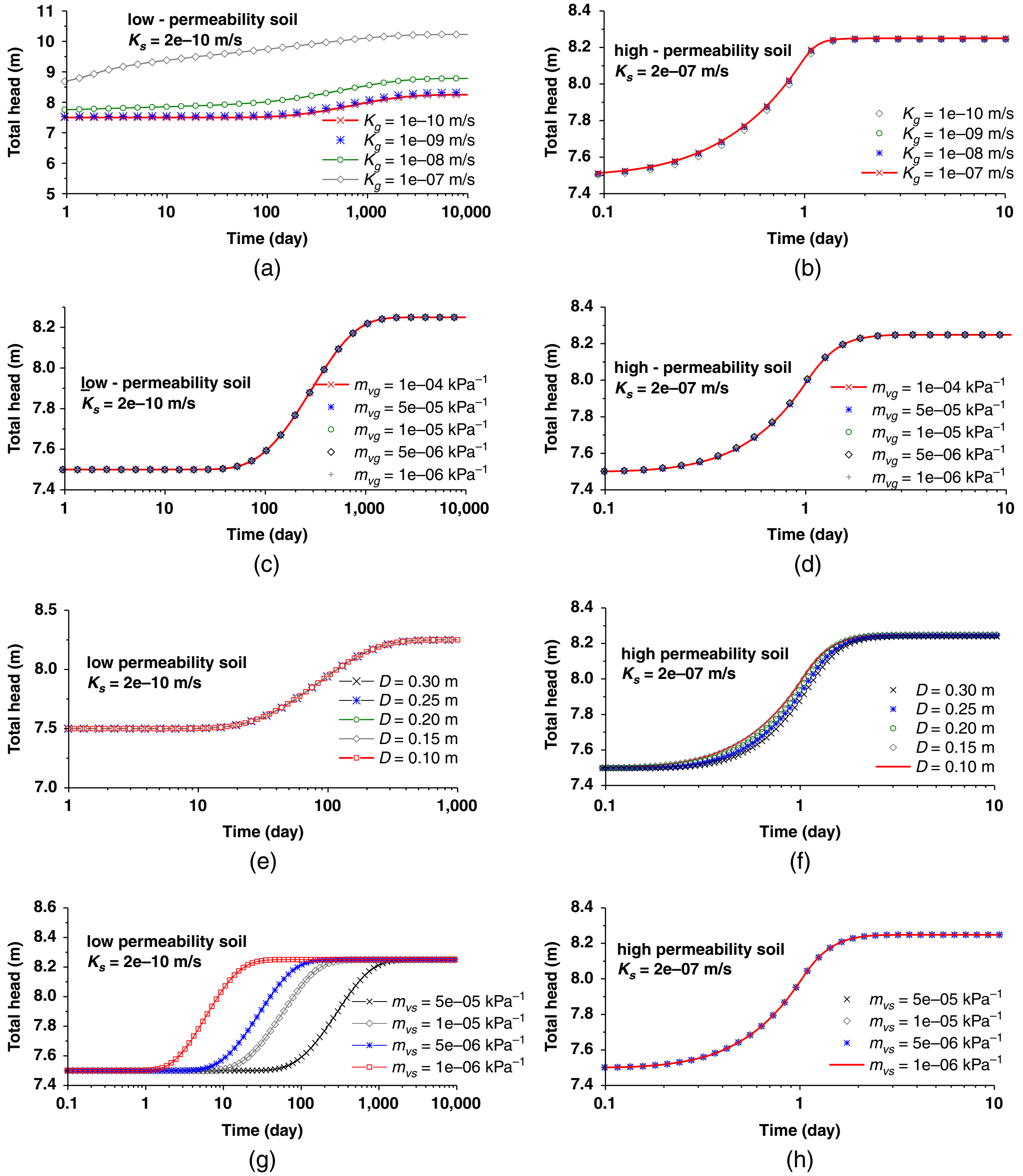

TABLE 4

Soil and grout properties included in scenario 2.

Soil	K_s, m/s	m_{vs}, kPa^{-1}	G	K_g, m/s	m_{vg}, kPa^{-1}	K_g/K_s ($K_s = 2.0 \times 10^{-10}$, m/s)	K_g/K_s ($K_s = 2.0 \times 10^{-9}$, m/s)
1	2.0×10^{-10}	1.49×10^{-6}	1	2.0×10^{-10}	1.49×10^{-5}	1	0.1
2	2.0×10^{-9}	1.49×10^{-5}	2	2.0×10^{-9}	1.49×10^{-5}	10	1
–	–	–	3	2.0×10^{-8}	1.49×10^{-5}	100	10
–	–	–	4	2.0×10^{-7}	1.49×10^{-5}	1,000	100
–	–	–	5	2.0×10^{-6}	1.49×10^{-5}	10,000	1,000

conditions for a vertical stress increment at the soil surface. An external uniform load of 100 kPa was applied on a circular surface with a diameter of 8 m at the surface of a clay layer. The clay layer thickness was extended to 20 m to minimize possible boundary issues, if any. The borehole has a diameter of 100 mm. It penetrates within the clay layer over a depth of 16 m. The external loading induced an excess pore water pressure (EPWP) in the soil. Fully grouted piezometers were defined under the center of the circular surface load to monitor the EPWP evolution versus borehole depth up to 15 m. SIGMA/W (GEO-SLOPE International Ltd. 2013) and SEEP/W were used in a coupled analysis to simulate the EPWP caused by the external load and its dissipation. In this case, SIGMA/W solves a series of static equilibrium and stress-strain equations, while SEEP/W solves Richards' (1931) equation.

Soil and grout were treated as linear-elastic materials with effective-stress parameters. Four types of low-permeability soil were included in this scenario. Their K_s values ranged between 2×10^{-9} and 2×10^{-10} m/s. Their Young's modulus (E_s) ranged between 5 and 50 MPa. For this problem, ten types of grout were included in the model, with K_g ranging between 2×10^{-6} and 2×10^{-10} m/s, and E-modulus ranging between 5 and 500 MPa. All soil and grout types have the same arbitrary values of ν and unit weight of 0.3 and 20 kN/m^3, respectively. Table 5 summarizes the soil and grout properties for this model.

FIG. 5

Sketch of the fully grouted piezometers and loading with contours of the vertical stress increment in soil.

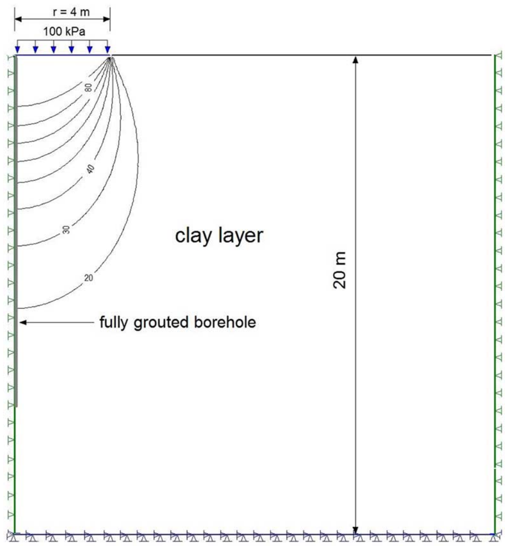

TABLE 5
Soil and grout properties included in scenario 3.

Soil	K_s, m/s	E_s, MPa	G	K_g, m/s	E_g, MPa	G	K_g, m/s	E_g, MPa
1	2.0×10^{-10}	50	1	2.0×10^{-10}	5	6	2.0×10^{-10}	500
2	2.0×10^{-10}	5	2	2.0×10^{-9}	5	7	2.0×10^{-9}	500
3	2.0×10^{-9}	50	3	2.0×10^{-8}	5	8	2.0×10^{-8}	500
4	2.0×10^{-9}	5	4	2.0×10^{-7}	5	9	2.0×10^{-7}	500
–	–	–	5	2.0×10^{-6}	5	10	2.0×10^{-6}	500

The simulation was conducted in two steps. Step 1 simulated in situ ground conditions before applying the mechanical load. The in situ condition was defined by applying a groundwater table at the top boundary of the model to generate the initial PWP condition. In step 2, a uniform surface pressure was applied as a normal stress versus time boundary condition using the step function. A surface load increment of 100 kPa was applied from $t = 0$ to $t = 1$ day. The surface pressure was kept constant for the remaining duration of the simulation (730 days). The total stress increment along the vertical axis of symmetry obtained by SIGMA/W was compared to the stress increase given by the Foster and Ahlvin (1954) influence chart for a uniform circular footing. A good agreement between the numerical and analytical solutions was obtained. The stress contour for a vertical stress increment of 30 kPa (30 %) intercepts the vertical centerline at a depth of around 8 m, the diameter of the circular loading surface (Fig. 5). More than 40 numerical simulations were completed to assess the performance of the fully grouted piezometers under the external load.

Mesh and Time-Stepping Parameters

Numerical solution accuracy depends upon the mesh size and time-step increments. Using a coarse mesh can produce an inaccurate numerical solution. At the same time, using a very fine mesh increases the computation time. Thus, nonuniform mesh refinement is often preferable. The mesh should be refined where local changes in hydraulic head and hydraulic gradient are more abrupt. The solution should also be mesh independent (Chapuis 2010, 2012a, 2012b, 2012c). A mesh containing 14,023 elements was used for scenarios 1 and 2. For scenario 3, the mesh contained 23,247 elements. The mesh has 0.5-cm elements at the interface of the fully grouted borehole and the clay layer, and 50-cm elements far away from the borehole.

For transient analyses, the time-step increments must result in a solution that is time-step independent. Exponential time steps are often used for well hydraulic simulations. For scenarios 1 and 2, several time-stepping schemes with time steps increasing exponentially from 10, 100, 1,000, and 3,600 s were found to provide similar PWP responses. Consequently, an initial time step of 3,600 s was used. The initial time step was set to 0.9 day for the SIGMA/W model.

Results

FIELD PERFORMANCE OF FULLY GROUTED PIEZOMETERS

Fig. 6 presents the changes in atmospheric inputs (i.e., barometric pressure and total precipitation), groundwater level in the upper aquifer (i.e., upper boundary of the clay layer), and PWP in the lower portion of the intact clay. Changes in atmospheric pressure were

FIG. 6 Pore pressure and atmospheric inputs for the field site. (a) Barometric fluctuations and total precipitation; (b) groundwater level changes in the upper aquifer; (c) raw and corrected PWP in the lower portion of the clay, registered by fully grouted piezometer F1B sealed with grout G1 ($K_g = 6.1 \times 10^{-9}$ m/s); and (d) raw and corrected PWP in the lower portion of the clay, registered by fully grouted piezometer F3B sealed with grout G3 ($K_g = 1.2 \times 10^{-6}$ m/s).

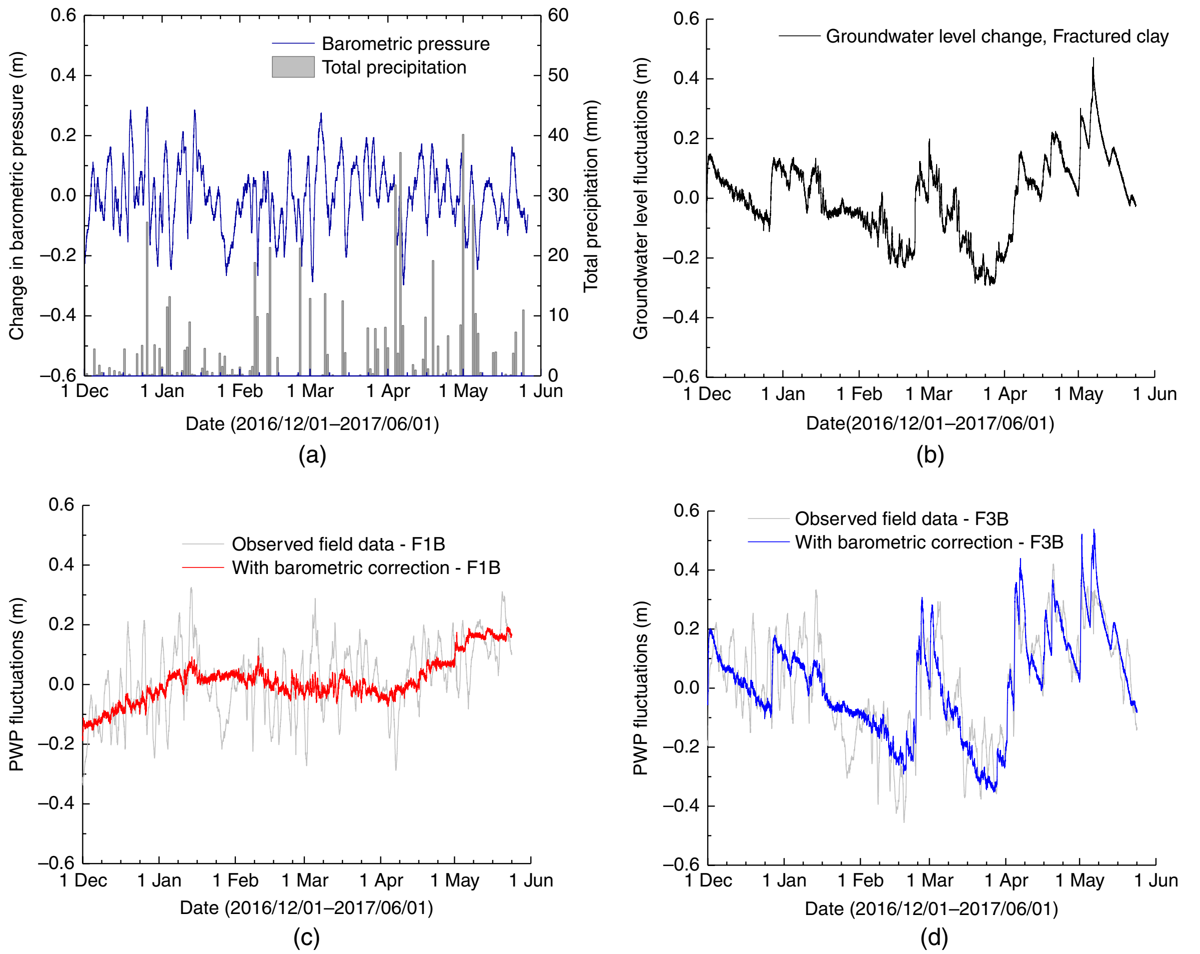

obtained from a weather station installed 2 km away from the study site by the hydrology research group of École de technologie supérieure. The groundwater level fluctuations were recorded using a pressure transducer (full-scale range of 100 kPa) installed in a standpipe piezometer that was completed below the groundwater level in borehole F2. The PWP fluctuations were measured by the fully grouted VWPs. All field data were automatically logged at intervals of 15 min between November 2016 and June 2017.

During the study period, the mean value for the barometric pressure expressed as an equivalent water column was 10.22 m (Fig. 6a). The barometric pressure fluctuated from −0.29 to +0.30 m around the mean (i.e., a total variation of 0.59 m). This range represents the amplitude of the groundwater level and PWP changes due to barometric pressure. These fluctuations are large enough to conceal the PWP changes caused by other natural loadings. Thus, the PWP fluctuations caused by the barometric pressure changes must be removed from the groundwater level and PWP data. The multiple regression technique described in Marefat, Duhaime, and Chapuis (2015) and Marefat (2016) was used to correct the PWP data for barometric effect. Fig. 6c and d presents both raw and corrected PWP data observed in the lower part of the clay layer with the two fully grouted VWPs. Even if a major part of the fluctuations were removed from the data, there are still some minor fluctuations in the barometric corrected data. These minor high-frequency fluctuations might be related to earth tides or some other unknown transients. In addition, the barometric pressure was measured at about 2 km away from the test site. This may cause some inaccuracy when correcting the PWP for the barometric pressure.

The minor high-frequency fluctuations can be filtered using a low-pass filtering technique. A low-pass filter with a cutoff frequency of 0.3 day^{-1} was applied to the data corrected for barometric pressure to remove the high-frequency fluctuations. The filtered data series shown in Fig. 7 were obtained using the signal processing toolbox in MATLAB (MathWorks, Natick, MA).

As shown in Fig. 7, the piezometers' responses exhibit a number of hydrologic patterns. First, during the monitoring period, the groundwater level in the upper aquifer (fractured clay) shows several hydraulic head peaks. These fluctuations in total head within the shallow aquifer depend upon rain and snow melting events. Secondly, in the lower portion of the clay layer, the PWP responses of fully grouted piezometers F1B and F3B differed significantly from each other. The response of F3B, backfilled with grout G3 ($K_g = 1.2 \times 10^{-6}$ m/s), directly mimics the groundwater level change in the upper fractured clay. This implies a direct hydraulic connection between the fully grouted piezometer and the upper aquifer. As mentioned earlier, grout G3 and the surrounding clay have a K_g/K_s ratio of around 1,100. This ratio causes a hydraulic short circuit between the piezometer and the upper aquifer. The permeability ratio of 1,100 was obtained based on laboratory tests on small specimens taken from the grout before the piezometer installation. Because of segregation and scale effects, this ratio may not be representative. Some parts of the PWP time series show higher peaks for the F3B response compared to the response for the fractured clay. This may be due to water accumulation in the upper part of borehole F3, as the annular space was free of grout because of the segregation and sedimentation that occurred immediately after the setting of grout G3. The fully grouted piezometer in borehole F3B responded to this supplementary water column. However, piezometer F1B,

FIG. 7

Field data corrected for barometric pressure and high-frequency transients. The groundwater level was measured within a standpipe in the upper fractured clay. The PWP was measured within the intact clay layer with two fully grouted VWPs using grouts G3 ($K_g = 1.2 \times 10^{-6}$ m/s) for F3B and G1 ($K_g = 6.1 \times 10^{-9}$ m/s) for F1B.

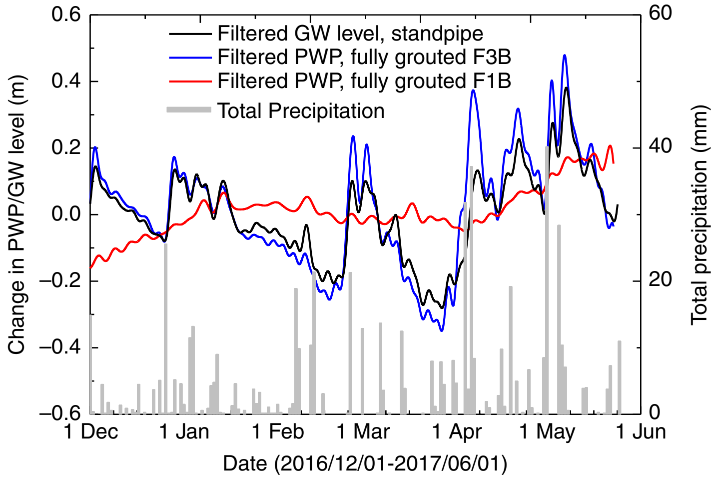

backfilled with grout G1 ($K_g = 6.1 \times 10^{-9}$ m/s), monitored a smooth and dampened pore pressure response as expected for an intact clay layer. The seasonal groundwater fluctuations applied at the top boundary of the clay layer are dampened and delayed while they propagate downward into the clay layer.

FULLY GROUTED PIEZOMETER RESPONSE TO A 1-DAY CHANGE IN GROUNDWATER LEVEL

Fig. 8 shows equipotentials for the first numerical modeling scenario. Equipotentials are shown for a period of 50 days after a change in the groundwater level for soil 1 ($K_s = 2 \times 10^{-10}$ m/s) and for grouts with K_g values between $10K_s$ and $10{,}000K_s$. The hydraulic head distribution around the borehole changes if there is a high contrast in hydraulic conductivity between grout and surrounding formation. As shown in Fig. 8e, the hydraulic head at the bottom of the borehole is similar to that obtained at the upper boundary of the clay layer. This is a consequence of the hydraulic short circuit between the borehole and the upper aquifer. On the other hand, with soil 4 ($K_s = 2 \times 10^{-7}$ m/s) and grouts with K_g values between $0.001K_s$ and $10K_s$, the numerical results show that the grout hydraulic conductivity has no influence on the hydraulic head distribution around the borehole (not shown here).

Fig. 9a and b presents the PWP equalization for fully grouted piezometers installed at a depth of 5 m within the soil. In soil 1 ($K_s = 2 \times 10^{-10}$ m/s), for K_g values of K_s and $10K_s$, the pore pressure response of the fully grouted piezometers matches the response of the reference piezometer. For $K_g/K_s \geq 10$, the fully grouted piezometer response differs from the reference piezometer. For a higher hydraulic conductivity ratio ($K_g/K_s \geq 100$), the borehole acts as a conduit for groundwater flow. In soils 3 and 4, for all grouts, the PWP responses match the response of the reference piezometer. As shown in Fig. 9c and d, using a low-permeability grout did not induce a time lag for the fully grouted piezometer.

The influence of grout compressibility on the PWP response was also investigated (Fig. 10). For the borehole geometry modeled in this study ($D = 100$ mm), grout compressibility has no important influence on the response of fully grouted piezometers. Grout compressibility has a slight influence on the very early PWP response in soil 1 for high-permeability grout ($K_g/K_s \geq 1{,}000$) and in soil 4 for a low-permeability grout ($K_g/K_s \leq 0.001$).

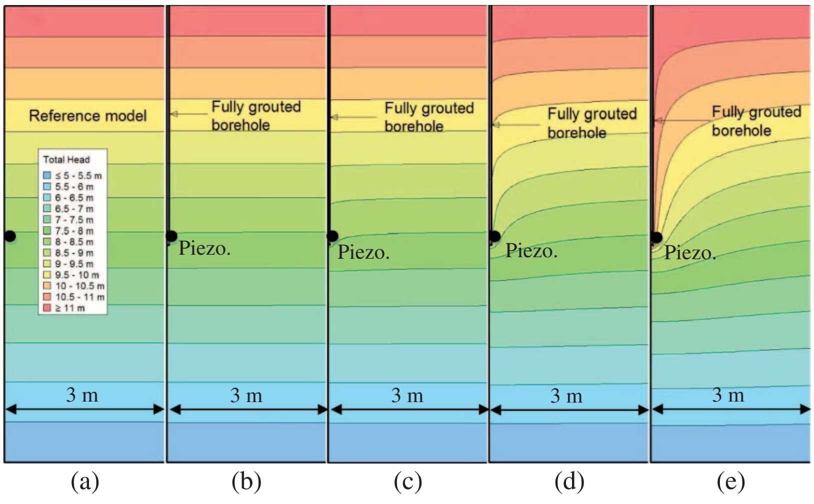

FIG. 8 Comparison of equipotentials for reference model and fully grouted piezometers for scenario 1 and soil 1, $K_s = 2 \times 10^{-10}$ m/s and $m_{vs} = 1.49 \times 10^{-5}$ kPa^{-1}. (a) Reference model, (b) fully grouted piezometer, $K_g/K_s = 10$, (c) fully grouted piezometer, $K_g/K_s = 100$, (d) fully grouted piezometer, $K_g/K_s = 1{,}000$, and (e) fully grouted piezometer, $K_g/K_s = 10{,}000$. All grouts have an m_{vg} of 1.49×10^{-5} kPa^{-1}.

FIG. 9 Comparison of the pore pressure response for fully grouted and reference piezometers. (a) Soil 1, $K_s = 2 \times 10^{-10}$ m/s, (b) soil 2, $K_s = 2 \times 10^{-9}$ m/s, (c) soil 3, $K_s = 2 \times 10^{-8}$ m/s, and (d) soil 4, $K_s = 2 \times 10^{-7}$ m/s. All soils and grouts have a compressibility of 1.49×10^{-5} kPa^{-1}.

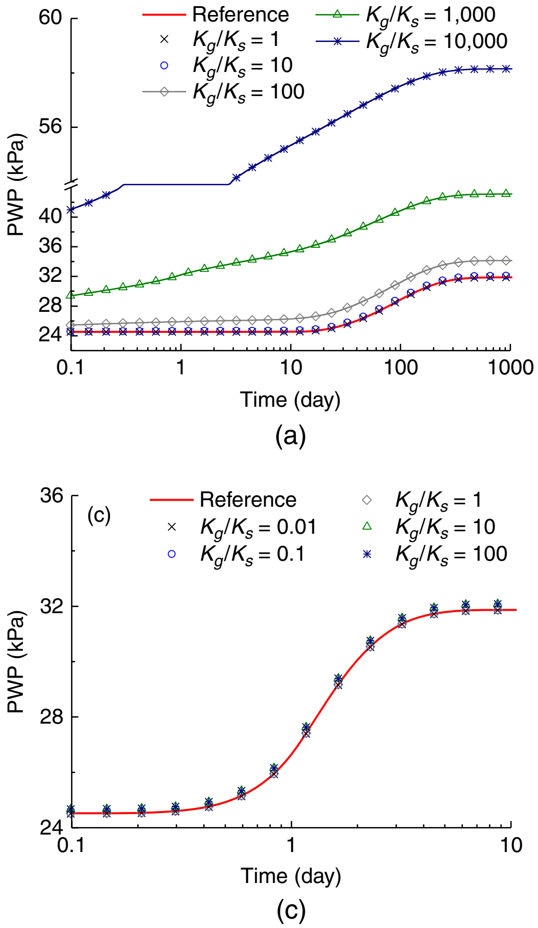

The normalized error was calculated for each fully grouted piezometer with respect to the reference piezometer data. Fig. 11 presents the normalized error ε versus K_g/K_s. To calculate ε based on Eq 1, u_t^* is the pore pressure measured with the reference model (e.g., Fig. 8a) and u_{tfg} is the pore pressure measured with the fully grouted piezometer (e.g., Fig. 8b–e). The ε values for K_g/K_s ratios between 10^{-3} and 10 are very small. The ε value is greater at higher K_g/K_s ratios. These higher ratios correspond to the simulations with low-permeability soils 1 and 2. For $K_g/K_s = 1{,}000$, a normalized error of about 35 % was obtained. Fig. 9 also shows that the grout compressibility has no significant effect on the ϵ values.

FULLY GROUTED PIEZOMETER RESPONSE TO A SEASONAL CHANGE IN GROUNDWATER LEVEL

Fig. 12 presents the response to a seasonal fluctuation in the groundwater level of a fully grouted piezometer installed at a depth of 5 m in soil 1 ($K_s = 2 \times 10^{-10}$ m/s) and soil 2 ($K_s = 2 \times 10^{-9}$ m/s). For the reference piezometer (natural condition), when

FIG. 10 Influence of grout compressibility on the PWP response. (a) Soil 1, $K_s = 2 \times 10^{-10}$ m/s, and (b) soil 4, $K_s = 2 \times 10^{-7}$ m/s.

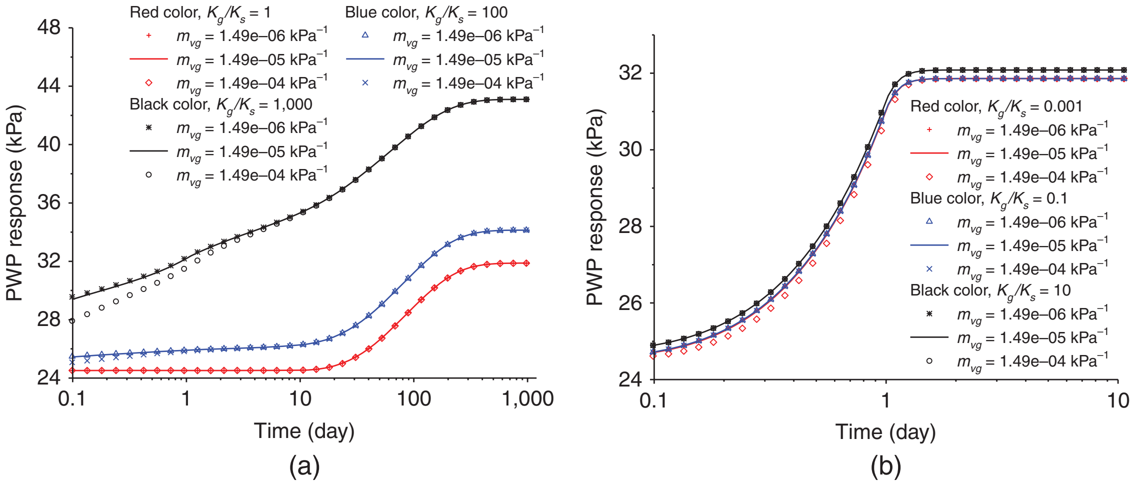

FIG. 11

Normalized error for fully grouted piezometers with respect to reference piezometers for scenario 1.

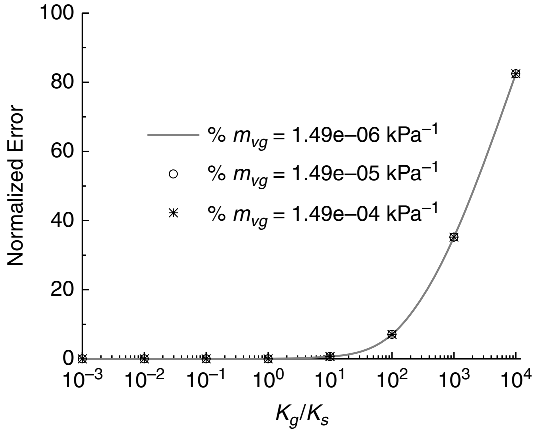

$K_s = 2 \times 10^{-10}$ m/s, the response is delayed and dampened when compared to that for $K_s = 2 \times 10^{-9}$ m/s. The nearly constant response of the reference piezometer is related to the fact that the seasonal head fluctuation at the upper boundary of the low-permeability soil is dampened while propagating downward into the soil. For a ratio of $K_g/K_s \leq 100$, there is a good correlation between the fully grouted and reference piezometers. This smooth and dampened response is consistent with the response of piezometer F1B in Sainte-Marthe. This piezometer was sealed with low-permeability grout G1. For $K_g/K_s \geq 100$, the response of fully grouted piezometers differs from that of the reference piezometer. For a higher hydraulic conductivity ratio, the fully grouted piezometer response replicates the groundwater table fluctuations. For $K_g/K_s \geq 1{,}000$, the hydraulic connection between the piezometer and the upper boundary is obvious. The hydraulic connection between the fully grouted piezometer and the upper boundary of the clay

FIG. 12

Fully grouted piezometer response for seasonal groundwater fluctuations. (a) Soil 1,$K_s = 2 \times 10^{-10}$ m/s, and (b) soil 2, $K_s = 2 \times 10^{-9}$ m/s.

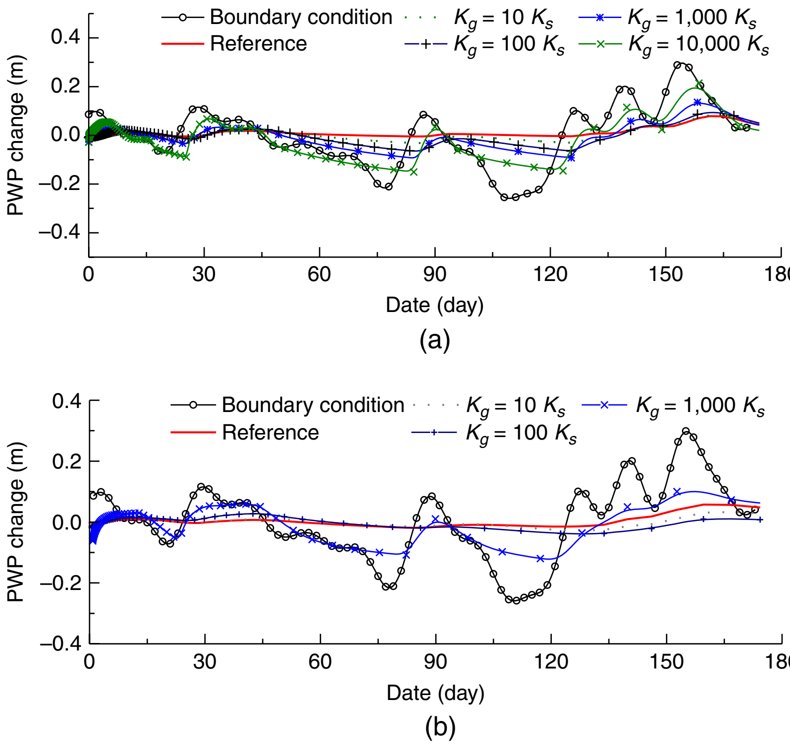

matches the response observed for piezometer F3B in Sainte-Marthe. Piezometer F3B was also sealed with a high-permeability grout (G3).

FULLY GROUTED PIEZOMETER RESPONSE TO AN EXTERNAL MECHANICAL LOADING

Fig. 13 presents the EPWP versus borehole depth for fully grouted and reference piezometers installed in a clay layer with $K_s = 2 \times 10^{-10}$ m/s and $E_s = 5$ MPa. The EPWP data along the borehole centerline are presented for 5, 50, 200, and 730 days after loading. As shown in Fig. 13, for K_g values of K_s and $10K_s$, the fully grouted piezometer responses correlate well with the response of the reference piezometer for all borehole depths. For high values of the hydraulic conductivity ratio ($K_g/K_s > 100$), fully grouted piezometers do not provide accurate measurements for the initial EPWP generation at the shallow depth where the initial EPWP reaches a maximum value (Fig. 13a and b). Using a very high-permeability grout ($K_g/K_s \geq 1{,}000$) in the borehole accelerates the dissipation of the EPWP. The borehole acts as a vertical drain.

Fig. 13 shows that the influence of the permeability ratio on the piezometer response to the surface loading depends on the piezometer depth and the time elapsed since loading. After loading, the initial EPWP at shallow depths dissipates quickly if the borehole is sealed with a very high-permeability grout. For such a shallow piezometer, the permeability ratio between grout and surrounding soil becomes critical. Accordingly, at shallow depth, a fully grouted piezometer sealed with very high-permeability grout does not show an accurate EPWP. This is not the case for deep piezometers, for which the permeability ratio is less

FIG. 13 Excess PWP versus depth, soil with $K_sE_s = 1 \times 10^{-6}$ m^2/s ($K_s = 2 \times 10^{-10}$ m/s and $E_s = 5$ MPa). (a) After 5 days of loading, (b) after 50 days of loading, (c) after 200 days of loading, and (d) after 730 days of loading.

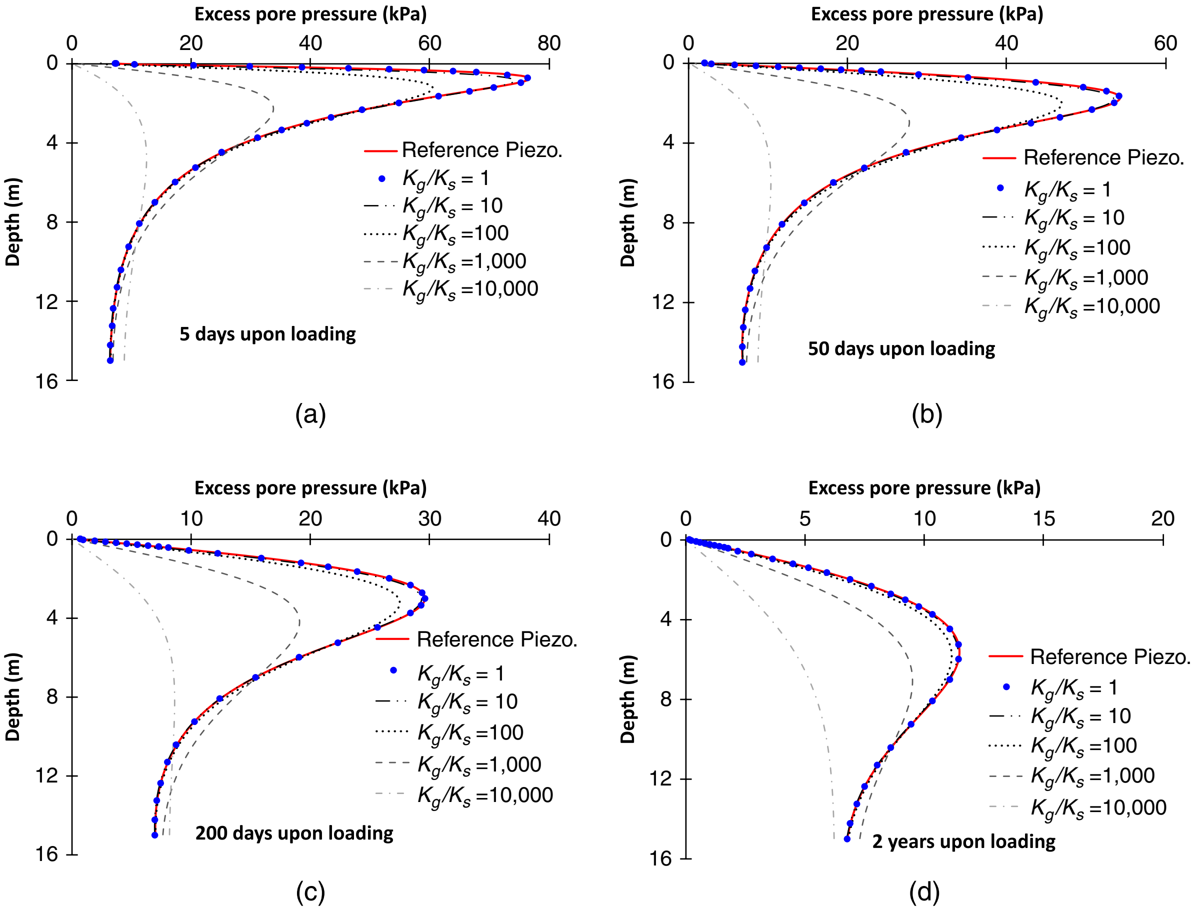

critical. As shown in Fig. 13a and b, after 5–50 days of loading, all piezometers underneath 8 m provided similar EPWP measurements and were insensitive to the permeability ratio. Yet with longer time, the permeability ratio becomes important at progressively greater depths (Fig. 13c and d). This finding is in agreement with previous results presented by the authors that show that piezometer depth influences the piezometric error induced by a steady-state seepage condition (Marefat, Chapuis, and Duhaime 2014).

The influence of grout stiffness on the EPWP induced by the external load was studied numerically. Soft ($E = 5$ MPa) and stiff ($E = 500$ MPa) grouts provided similar EPWP responses (not shown here). The results showed that, for a borehole with a diameter of around 100 mm, the grout stiffness has no significant influence on the response of fully grouted piezometers.

Discussion

The fully grouted method for piezometer installation has one main disadvantage that is often overlooked: preparing a low-permeability grout for soft clay is less trivial than it might seem. Recipes for grout in soft and stiff clay have already been discussed by Mikkelsen (2002) and Contreras, Grosser, and Ver Strate (2007, 2008). These recipes provide stable grouts if consistency is adjusted with additional bentonite. A successful fully grouted installation in a low-permeability soil requires a grout that is similar to the soil in terms of hydraulic conductivity and stiffness values. Stiffness and strength are controlled by the water-cement (w/c) ratio. The bentonite and cement contents control the grout permeability. The addition of more bentonite lowers the permeability and increases the viscosity, but too much bentonite produces a grout that is too viscous to easily flow into narrow spaces in the borehole. Adding more cement also lowers the permeability and increases its final strength. Adding more cement during grout mixing is undesirable because of a risk of flash set and because a lower w/c ratio can make the grout too strong for the soil conditions.

Numerical and field experiments were presented in this article regarding the performance of fully grouted piezometers under various transient conditions. They demonstrated that fully grouted piezometers produce accurate PWP measurements. However, certain criteria must be respected regarding the properties and physical stability of the liquid grout. Our results have shown that the hydraulic conductivity and stiffness of the soil and the hydraulic conductivity of the grout are the most important parameters to obtain an accurate PWP response. According to the numerical results, in a soil with $K \geq 2 \times 10^{-8}$ m/s, all types of grout can be used to grout the piezometer. For the borehole geometry modeled in this article, a very low-permeability grout, with $K_g/K_s = 0.001$, did not induce any time lag.

Our field experiment showed that grout physical stability is another important parameter when using the fully grouted method. The grout initial viscosity (consistency) controls its physical stability. To produce a physically stable grout mix, its initial viscosity should be verified. This finding confirms previous results on grout stability by Contreras, Grosser, and Ver Strate (2007, 2008). An easy method to measure and control the viscosity in the field is the Marsh Funnel viscosity test, as described in ASTM D6910-09, *Standard Test Method for Marsh Funnel Viscosity of Clay Construction Slurries*. The authors have experienced that a grout with a Marsh Funnel viscosity between 40 and 100 s is not only physically stable but also pumpable. Contreras, Grosser, and Ver Strate (2007) also proposed a narrower range for Marsh Funnel viscosity between 50 and 60 s.

The numerical simulations assumed a grout compressibility ranging from 1.49×10^{-6} to 1.49×10^{-4} kPa (E between 5 and 500 MPa). The numerical results showed that grout compressibility has little influence on the PWP response. However, grout stiffness is important in terms of good long-term performance of the fully grouted piezometer. Using a stiff grout in soft soils is not recommended (e.g., McKenna 1995). Stiff grout may crack, which causes a hydraulic short circuit and affects the piezometer reading. It is important to note here that a borehole with a diameter of 100 mm (~4 in.) was modeled. This borehole diameter is similar to some commonly used borehole diameters (i.e., 114 mm for HW casing) for piezometer installation. The influence of grout compressibility on the performance of fully grouted piezometers installed in boreholes with a diameter that is significantly larger than 100 mm needs to be investigated.

The boreholes in this study were shallow (less than 30 m). Hence, borehole grouting was completed using a single grout for each borehole. Nevertheless, for deep boreholes, staged grouting should be applied to avoid over-pressurizing the transducers during the installation (Contreras, Grosser, and Ver Strate 2007). Staged grouting can also be a good practice for the installation of fully grouted piezometers in a stratified soil in which large permeability contrasts are present. In this case, various types of grout with different permeability values can be pumped through multiple grout pipes down to the target formation. If staged grouting is not selected for the installation of a fully grouted piezometer in layered soil, the lowest permeability controls the installation (Contreras, Grosser, and Ver Strate 2007, 2011).

Our field observations and the numerical results imply that the previous findings of Vaughan (1969) are true but that the Contreras, Grosser, and Ver Strate (2007, 2008) results might only be true under certain circumstances. The results of this study demonstrated that $K_g = 100K_s$ is the upper limit to obtain acceptable PWP responses in the low-permeability soils ($2 \times 10^{-10} \leq K_s \leq 2 \times 10^{-9}$ m/s) that were modeled in this study. The numerical results have shown that using a high-permeability grout with $K_g/K_s \geq 1{,}000$ resulted in a PWP response that differed totally from the reference piezometer data. A K_g/K_s ratio between 0.001 and 10 provided accurate PWP and EPWP measurements for all soils modeled in this study. A comparison of the three scenarios of this study showed that the permeability ratio is less critical for deep piezometers under surface mechanical loading (scenario 3 in this study). The field observations have shown that using a low-permeability grout with $K_g/K_s \leq 10$ resulted in a precise PWP response. However, a permeability ratio of $K_g/K_s \geq 1{,}000$ resulted in a PWP response that mimics the changes in groundwater table elevation in the top fractured clay.

Our experience with the grout recipe for soft soils stresses the importance of adjusting the grout viscosity with additional bentonite, as suggested by Mikkelsen (2002) and Contreras, Grosser, and Ver Strate (2007, 2008). The base recipe for soft soils (6.55 parts water: 1 part cement: 0.4 part bentonite) without adding extra bentonite for viscosity adjustment was unstable in the field and in the laboratory. A quantitative method to adjust bentonite content in the field or a new grout recipe having a similar permeability and stiffness as the Champlain clay is required to improve the installation of fully grouted piezometers in soft soils. This is one of the objectives of a laboratory testing program on the properties of cement-bentonite grouts that is currently underway at École de technologie supérieure.

Conclusion

The fully grouted technique not only simplifies installation procedures but also has many other advantages. It reduces the installation time and cost, eliminates the risk of failure for the sand pack of deep wells, and makes piezometer installation easier. In this article, through a field experiment and numerical modeling, the influence of various parameters on the response of fully grouted piezometers under transient conditions was investigated. The results indicated that fully grouted piezometers allow accurate PWP responses to be measured. However, certain criteria should be respected. The piezometers' responses are strongly related to the hydraulic conductivity ratios between the grout and surrounding soil. This ratio is especially important for low-permeability soils, as devising recipes for low-permeability grouts is not as trivial as it might seem.

Baseline pore pressure monitoring in Sainte-Marthe clay demonstrated that using an improperly formulated grout resulted in an improper seal and a hydraulic connection to the upper aquifer. Although laboratory tests showed a K ratio of 1,100, the field ratio could be higher. However, the piezometer that was sealed using a grout with $K_g/K_s \leq 10$ resulted in a smooth and dampened response, as expected for an intact clay deposit.

The permeability ratios reported in this article were obtained based on small-scale laboratory tests. The field values may include some scale effect. The numerical studies also provided a consistent result with respect to the field observation. For a low-permeability soil with K between 2×10^{-10} and 2×10^{-9} m/s, using a grout with a K_g/K_s ratio of 1,000 resulted in a response that differed greatly from the reference piezometer response. For the soils modeled in this study, the numerical results provided an upper limit for K_g/K_s of 100 to measure an accurate PWP. Because of grout segregation, the field test for the high-permeability grout was inconclusive.

Our field and laboratory results indicate that K_g is the dominant factor that controls the fully grouted piezometer response. Besides K_g, the physical stability of the liquid grout is a critical factor. For the borehole geometry modeled here, a very low-permeability grout did not induce any time lag. For the soil and borehole geometries modeled in this study, the grout stiffness does not influence the performance of fully grouted piezometers. However, the grout stiffness is important for a good long-term performance of the grout. Stiffness is most important with soft soil. If the grout column is stiffer than the ground, the grout could crack and open up undesirable hydraulic paths. It is better to match the soil stiffness or err on the less stiff side.

ACKNOWLEDGMENTS

The authors would like to acknowledge the contribution of NSERC and GKM Consultants to the funding of this research project and of the Municipality of Sainte-Marthe for granting access to the test site. The editor and three anonymous reviewers deserve thanks for their helpful comments and suggestions.

References

ASTM D4767, 2011, *Standard Test Method for Consolidated Undrained Triaxial Compression Test for Cohesive Soils*, ASTM International, West Conshohocken, PA, www.astm.org

ASTM D5084, 2016, *Standard Test Methods for Measurement of Hydraulic Conductivity of Saturated Porous Materials Using a Flexible Wall Permeameter*, ASTM International, West Conshohocken, PA, www.astm.org

ASTM D6910, 2009, *Standard Test Method for Marsh Funnel Viscosity of Clay Construction Slurries*, ASTM International, West Conshohocken, PA, www.astm.org

Bayrd, G., 2011, "Evaluating Practices for Installation of Vibrating Wire Piezometers," *Geotech. News*, Vol. 27, No. 4, pp. 26–29.

Chapuis, R. P., 2009, "Monitoring a Well in a Clay Layer: Revisiting the Time Lag Problem," *Bull. Eng. Geol. Environ.*, Vol. 68, No. 3, pp. 387–395, https://doi.org/10.1007/s10064-009-0210-5

Chapuis, R. P., 2010, "Influence of Element Size in Numerical Studies of Seepage: 1. Large-Scale or Regional Studies," *Geotech. News*, Vol. 28, No. 4, pp. 31–34.

Chapuis, R. P., 2012a, "Influence of Element Size in Numerical Studies of Seepage: 2. Small-Scale Details," *Geotech. News*, Vol. 30, No. 1, pp. 32–35.

Chapuis, R. P., 2012b, "Influence of Element Size in Numerical Studies of Seepage: 3. Unsaturated Zones, Steady-State," *Geotech. News*, Vol. 30, No. 3, pp. 27–30.

Chapuis, R. P., 2012c, "Influence of Element Size in Numerical Studies of Seepage: 4. Unsaturated Zones, Transient Conditions," *Geotech. News*, Vol. 30, No. 4, pp. 34–37.

Contreras, I. A., Grosser, A. T., and Ver Strate, R. H., 2007, "The Use of the Fully-Grouted Method for Piezometer Installation," presented at the *Seventh International Symposium* *on Field Measurements in Geomechanics, FMGM 2007*, Boston, MA, American Society of Civil Engineers, Reston, VA.

Contreras, I. A., Grosser, A. T., and Ver Strate, R. H., 2008, "The Use of the Fully-Grouted Method for Piezometer Installation," *Geotech. News*, Vol. 26, pp. 30–37.

Contreras, I. A., Grosser, A. T., Ver Strate, R. H., 2011, "Practical Aspects of the Fully-Grouted Method for Piezometer Installation," presented at the *Eighth International Symposium on Field Measurements in Geomechanics, FMGM*, Berlin, Germany.

Contreras, I. A., Grosser, A. T., and Ver Strate, R. H., 2012, "Update of the Fully-Grouted Method for Piezometer Installation," *Geotech. News*, Vol. 30, No. 2, pp. 20–25.

DeJong, J. T., Fritzges, M. B., Sellers, J. B., and McRae, J. B., 2004, "Pore Pressure Characterization of Geotechncial Experimentation Site Using Multilevel Vibrating Wire Piezometers," presented at the *57th Canadian Geotechnical Conference*, Quebec, Canada, Canadian Geotechnical Society, Richmond, Canada, pp. 17–24.

Duhaime, F., 2012, "Mesure de la Conductivité Hydraulique du Dépôt d'argile Champlain de Lachenaie, Québec: Théorie et Applications," Ph.D. thesis, École Polytechnique de Montréal, Montréal, Canada.

Duhaime, F. and Chapuis, R. P., 2014, "A Coupled Analysis of Cavity and Pore Volume Changes for Pulse Tests Conducted in Soft Clay Deposits," *Int. J. Numer. Anal. Methods Geomech.*, Vol. 38, No. 9, pp. 903–924, https://doi.org/10.1002/nag.2238

Duhaime, F., Chapuis, R. P., Marefat, V., and Benabdallah, E. M., 2017, "Influence of Seasonal Hydraulic Head Changes on Slug Tests Conducted in Shallow Low-Permeability Soils," *Eng. Geol.*, Vol. 228, pp. 385–394, https://doi.org/10.1016/j.enggeo.2017.08.017

Foster, C. R. and Ahlvin, R. G., 1954, "Stresses and Deflections Induced by a Uniform Circular Load," presented at the *33rd Annual Meeting of the Highway Research Board*, Washington, DC, Highway Research Board, Washington, DC, pp. 467–470.

Geo-Slope International Ltd., 2012, *Seepage Modeling with SEEP/W: An Engineering Methodology*, GEO-SLOPE International Ltd., Calgary, Canada.

Geo-Slope International Ltd., 2013, *Stress-Deformation Modeling with SIGMA/W: An Engineering Methodology*, GEO-SLOPE International Ltd., Calgary, Canada.

Hvorslev, M. J., 1951, "Time-Lag and Soil Permeability in Ground Water Observations," *Bulletin No. 36*, U.S. Army Waterways Experiment Station, Vicksburg, MS, 50p.

Jurado, A., De Gaspari, F., Vilarrasa, V., Bolster, D., Sánchez-Vila, X., Fernàndez-Garcia, and Tartakovsky, D. M., 2012, "Probabilistic Analysis of Groundwater-Related Risks at Subsurface Excavation Sites," *Eng. Geol.*, Vol. 125, pp. 35–44, https://doi.org/10.1016/j.enggeo.2011.10.015

Marefat, V., 2016, "Natural Pore Pressure Fluctuations in a Champlain Clay Deposit," Ph.D. thesis, École Polytechnique de Montréal, Montréal, Canada.

Marefat, V., Chapuis, R. P., and Duhaime, F., 2014, "Piezometric Error for Fully Grouted Piezometers Installed in Clay Layers," presented at the *67th Canadian Geotechnical Conference*, Regina, Canada, Canadian Geotechnical Society, Richmond, Canada.

Marefat, V., Duhaime, F., and Chapuis, R. P., 2015, "Pore Pressure Response to Barometric Pressure Change in Champlain Clay: Prediction of the Clay Elastic Properties," *Eng. Geol.*, Vol. 198, pp. 16–29, https://doi.org/10.1016/j.enggeo.2015.09.005

McKenna, G. T., 1995, "Grouted-in Installation of Piezometers in Boreholes," *Can. Geotech. J.*, Vol. 32, No. 2, pp. 355–363, https://doi.org/10.1139/t95-035

Mikkelsen, P. E., 2000, "Grouting-in Piezometers," *Slope Indicator Co.*

Mikkelsen, P. E., 2002, "Cement-Bentonite Grout Backfill for Borehole Instruments," *Geotech. News*, Vol. 20, pp. 38–42.

Mikkelsen, P. E. and Green, G. E., 2003, "Piezometers in Fully Grouted Boreholes," presented at the *Sixth International Symposium on Field Measurements in Geomechanics, FMGM 2003*, Oslo, Norway, A. A. Balkema Publishers, Lisse, the Netherlands.

Pujades, E., Carrera, J., Vázquez-Suñé, E., Jurado, A., Vilarrasa, V., and Mascuñano-Salvador, E., 2012, "Hydraulic Characterization of Diaphragm Walls for Cut and

Cover Tunnelling," *Eng. Geol.*, Vol. 125, pp. 1–10, https://doi.org/10.1016/j.enggeo.2011.10.012

Pujades, E., Vázquez-Suñé, E., Carrera, J., Vilarrasa, V., De Simone, S., Jurado, A., Ledesma, A., Ramos, G., and Lloret, A., 2014, "Deep Enclosures versus Pumping to Reduce Settlements during Shaft Excavations," *Eng. Geol.*, Vol. 169, pp. 100–111, https://doi.org/10.1016/j.enggeo.2013.11.017

Richards, L. A., 1931, "Capillary Conduction of Liquids Through Porous Mediums," *Physics*, Vol. 1, No. 5, pp. 318–333, https://doi.org/10.1063/1.1745010

Simeoni, L., 2012, "Laboratory Tests for Measuring the Time-Lag of Fully Grouted Piezometers," *J. Hydrol.*, Vols. 438–439, pp. 215–222, https://doi.org/10.1016/j.jhydrol.2012.03.025

Simeoni, L., De Polo, F., Caloni, G., and Pezzetti, G., 2011, "Field Performance of Fully Grouted Piezometers," presented at the *Eighth International Symposium on Field Measurements in Geomechanics, FMGM*, Berlin, Germany.

Smerdon, B. D., Smith, L. A., Harrington, G. A., Gardner, W. P., Delle Piane, C., and Sarout, J., 2014, "Estimating the Hydraulic Properties of an Aquitard from In Situ Pore Pressure Measurements," *Hydrogeol. J.*, Vol. 22, No. 8, pp. 1875–1887, https://doi.org/10.1007/s10040-014-1161-x

Smith, L. A., van der Kamp, G., and Hendry, M. J., 2013, "A New Technique for Obtaining High-Resolution Pore Pressure Records in Thick Claystone Aquitards and Its Use to Determine In Situ Compressibility," *Water Resour. Res.*, Vol. 49, No. 2, pp. 732–743, https://doi.org/10.1002/wrcr.20084

Tavenas, F., Jean, P., Leblond, P., and Leroueil, S., 1983a, "The Permeability of Natural Soft Clays. Part II: Permeability Characteristics," *Can. Geotech. J.*, Vol. 20, No. 4, pp. 645–660, https://doi.org/10.1139/t83-073

Tavenas, F., Leblond, P., Jean, P., and Leroueil, S., 1983b, "The Permeability of Natural Soft Clays. Part I: Methods of Laboratory Measurement," *Can. Geotech. J.*, Vol. 20, No. 4, pp. 629–644, https://doi.org/10.1139/t83-072

Vaughan, P. R., 1969, "A Note on Sealing Piezometers in Boreholes," *Géotechnique*, Vol. 19, No. 3, pp. 405–413, https://doi.org/10.1680/geot.1969.19.3.405

Wan, M. S. P. and Standing, J. R., 2014, "Lessons Learnt from Installation of Field Instrumentation," *Proc. Inst. Civ. Eng. Geotech. Eng.*, Vol. 167, No. 5, pp. 491–506, https://doi.org/10.1680/geng.13.00054

Yungwirth, G., Preene, M., Dobr, M., and Forero Garcia, F., 2013, "Practical Application and Design Considerations for Fully Grouted Vibrating Wire Piezometers in Mine Water Investigations," presented at the *Annual International Mine Water Association Conference – Reliable Mine Water Technology*, Golden, CO, Publication Printers, Denver, CO, pp. 229–237.

Zawadzki, W. and Chorley, D., 2014, "Grouted-in Pressure Transducers: Implications for Hydrogeological Testing and Monitoring in Bedrock," *Mine Water Environ.*, Vol. 33, No. 3, pp. 289–292, https://doi.org/10.1007/s10230-014-0261-0